1-1-2023

Customer-based brand equity and customer behavioral intention: Evidence from insurance service

Elaheh Bakhshizadeh
Edith Cowan University

Hossein Aliasghari

10.5585/REMARK.V22I1.20256
Bakhshizadeh, E., & Aliasghari, H. (2023). Customer-based brand equity and customer behavioral intention: Evidence from insurance service. Brazilian Journal of Marketing, 22(1), 439-468. https://doi.org/10.5585/REMARK.V22I1.20256

Journal of Environmental Chemical Engineering 11 (2023) 109616

Contents lists available at ScienceDirect

Journal of Environmental Chemical Engineering

journal homepage: www.elsevier.com/locate/jece

Controlled synthesis of innovative carbon-based CaO_2 materials with boosted oxygen release performance in the aqueous environment

Chen Shen [a], Gang Wu [a], Jun Sun [a], Jinyu Hou [b], Hongqi Sun [c], Kuan Ding [a,*], Wuxing Liu [b], Shu Zhang [a]

[a] Joint International Research Laboratory of Biomass Energy and Materials, Jiangsu Co-Innovation Center of Efficient Processing and Utilization of Forest Resources, College of Materials Science and Engineering, Nanjing Forestry University, Nanjing 210037 Jiangsu, China
[b] Key Lab Soil Environment & Pollution Remediation, Institute of Soil Science, Chinese Academy of Sciences, No. 71, East Beijing Road, Nanjing 210008 Jiangsu, China
[c] School of Science, Edith Cowan University, 270 Joondalup Drive, Joondalup, WA 6027, Australia

ARTICLE INFO

Editor: <Yunho Lee>

Keywords:
Biochar
Oxygen release material
CaO_2
Groundwater pollution
Bioremediation

ABSTRACT

CaO_2 has been widely used as an oxygen-releasing material in bioremediation to improve the aerobe activity, but conventional encapsulation methods are difficult to control the oxygen-releasing rate and realize the full conversion of CaO_2. In this work, innovative biochar-loaded CaO_2 was prepared by an in-situ precipitation method. The biochars were modified using base-/acid-treatment to establish the relationship between the biochar properties and the oxygen releasing performance. Results indicated that increasing the oxygen content of biochars from 11% to 12% to ~20% caused a significant rise in CaO_2 loading amount from ~6 wt% to 13–14 wt%. The biochar with an average pore size equivalent to CaO_2 nanoparticle sizes (~12 nm) exhibited the longest oxygen-releasing time of 7.5 d, while the others presented shorter releasing periods of < 2.4 d. Meanwhile, a higher oxygen content of biochar triggered a decrease in the oxygen-releasing amount. Results from bioremediation experiments indicated that when comparing with the pure CaO_2 material, the optimized loading material (CaO_2 @BC800) nearly doubled the amount of bacteria while negligibly changed the pH of solution, giving a significant increase in the removal of diesel oil pollutant. Correspondingly, the in-situ loading on biochar can facilely regulate the oxygen-releasing performance and enhance the removal efficiency of bioremediation.

1. Introduction

Biochars are produced via the pyrolysis of biomass in an oxygen-limited or oxygen-free environment. Biochars are rich in carbon, with porous structure and abundant surface functional groups, and thus have good adsorption performance and chemical stability Zhang, Xing [62]. Therefore, in the field of environmental remediation, biochars have been widely used as adsorbents, amendments, slow-release fertilizer materials, and catalysts to remediate water and soil pollution [6,40,57]. For instance, Dike et al. found that biochars prepared at 900 °C mixed with fertilizer in the ratio of 1:9 can effectively repair diesel-polluted soil [10]. Kandanelli et al. use rice husk and sawdust to prepare biochars under different conditions without any physical or chemical modification, and the adsorption capacity of the biochar in the oil-water mixture reaches 2–3 g oil/g biochar [19]. Dong et al. load Fe_3O_4 on bamboo biochars to activate persulfate. After adding the catalyst, the degradation rate of persulfate on polycyclic aromatic hydrocarbons (PAHs) by persulfate increases from 14% to 86% Dong [13].

Chemical modification is a common method to modify the surface structure and chemical properties of biochars. In chemical modification, alkali treatment is usually used to obtain carbon materials with high specific surface area, while acid treatment is used to introduce oxygen-containing functional groups [47]. Wang et al. impregnated the biochar with 1 M HCl and NaOH. The specific surface area of the treated biochar doubled. FTIR showed that the -OH peak became stronger, indicating that the content of oxygen-containing functional groups was increased. The adsorption effect of the biochars treated with NaOH and HCl on carbendazim was 22% and 29% better than that of the untreated biochar, respectively Wang, Saleem [48]. Pan et al. treated biochars with nitric acid and phosphoric acid. The pore structure of the modified biochars was more developed, and the content of N and P in the carbon material was increased, so that it can provide more nutrients for the production of plants [36]. Wang used H_3PO_4 and KOH to modify biochars. The specific surface area of the modified carbon materials

* Corresponding author.
E-mail address: dingk@njfu.edu.cn (K. Ding).

https://doi.org/10.1016/j.jece.2023.109616
Received 20 December 2022; Received in revised form 21 February 2023; Accepted 28 February 2023
Available online 2 March 2023

increased by 10 times and 14 times respectively, and the adsorption capacity of enrofloxacin increased by 27.8% and 54.8% respectively [47,49].

On the other hand, the remediation of petroleum pollutants in groundwater, which originates from the accidental leakage of petroleum from pipelines and storage tanks, is currently an international research hotspot [39,42,52,64,65]. Among all the remediation technologies, bioremediation is a low-cost and green method without secondary pollution [45]. Many petroleum containment, such as polycyclic aromatic hydrocarbons (PAHs) [25], aliphatic hydrocarbons [27], and alkanes [58], could be effectively degraded to less harmful organic compounds or safe end products (like water and CO_2) by microorganisms [8]. During the practical application of biotechnology in groundwater remediation, the dissolved oxygen (DO) content plays a critical role in the remediation efficiency. For example, Yang et al. [60] find it takes only 12 h for monitoring well c (MWc) bacterial population to remove 99% of benzene at a DO concentration of 5 $mg{\cdot}L^{-1}$, but 24 h at 1 $mg{\cdot}L^{-1}$ [61]. Jasmann et al. use 3 V electrolysis to increase the DO concentration from 3 $mg{\cdot}L^{-1}$ to 11 $mg{\cdot}L^{-1}$, leading to the increased biodegradation rate of 1,4-dioxane from 68.7 $mg{\cdot}h^{-1}$ to 169 $mg{\cdot}h^{-1}$ Jasmann, Borch [17]. Park et al. use microorganism-encapsulated microbeads to degrade hydrocarbons, declaring that the degradation rate increases from 50% to 90.8% with adding oxygen from 1 $mg{\cdot}L^{-1}$ to 10.5 $mg{\cdot}L^{-1}$ [37]. The DO concentration plays a decisive role in the activity of aerobic bacteria, which further determines the degradation efficiency of petroleum in groundwater. The major reason is that molecular oxygen plays a triggering role as an electron acceptor in the activation of the carbon chain of alkanes or the aromatic ring of arenes [3,23]. Unfortunately, the groundwater environments are usually anoxic [4,38], which severely limits the efficiency of bioremediation (Zhou et al., 2022). As a result, increasing the DO content in groundwater is essential to enhance the bioremediation effectiveness of the oil containment.

In this regard, much effort has been made to use physical aeration and chemical oxygenation to improve the DO level in groundwater Khan [20]. However, the high oxygen releasing amount in a short time would cause an irreversible damage to cells. Among the applied technologies, chemical oxygen releasing materials have been commonly used due to the controllable oxygen release rate without disturbance of groundwater to expand pollution [34]. Among all the oxygen-releasing materials, CaO_2 shows the highest oxygen content and the lowest oxygen release rate, and therefore has attracted much attention Lu [28]. However, the reaction of CaO_2 with water results in a relatively rapid release of oxygen, leading to DO content exceeding the demand for microorganism aerobic degradation [66]. Accordingly, the preparation of CaO_2-based oxygen-releasing materials with a high oxygen-releasing capacity and a long releasing period is important for groundwater bioremediation.

Considering the properties of the biochars, they have been applied to improve the oxygen release performance of CaO_2 by a handful of researchers. First, biochars have prefect adsorption performance and chemical stability, enabling them to be used as carrier to load oxygen releasing agent CaO_2. Second, the porous structure of biochars can solve the problem of CaO_2 agglomeration and improve the oxygen release amount of CaO_2. On the other hand, the hydrophobicity and porous structure of biochars can affect the mass transfer effect of water, hinder the contact between water and CaO_2, and prolong the oxygen release time of CaO_2. In light of these, biochars are usually mixed with CaO_2 directly, or as a filler for encapsulating with CaO_2. Li et al. mix biochars with CaO_2 in water and then spread the obtained slurry in the river. The DO concentration of the overlying water of the river increases from 1.3 $mg{\cdot}L^{-1}$ to 2 $mg{\cdot}L^{-1}$ and remained at this concentration for 60 days [26]. However, simply blending with biochars can hardly improve the oxygen release performance of CaO_2. Wu et al. use polyvinyl alcohol to embed bamboo biochars and CaO_2 together to prepare biochar-based oxygen-releasing balls, and their oxygen release time is twice as long as those without bamboo biochars Wu [53]. Chang et al. employ a gelling agent (prepared with polyvinyl alcohol and alginate) to encapsulate CaO_2, biochars, rhamnolipid, and BTEX (benzene, toluene, ethylbenzene, and xylene) degrading bacteria to prepare oxygen-releasing balls and apply them to biodegradation. The BTEX degradation rate reaches 99% within 4 days Chang, Wang [5]. Nonetheless, encapsulating biochars with CaO_2 leads to problems such as the large volume of oxygen-releasing materials and low effective utilization of CaO_2. In particular, CaO_2 will react with water to form $Ca(OH)_2$, and the insoluble $Ca(OH)_2$ covered on the surface of CaO_2 will hinder the further reaction of internal CaO_2. As a result, the utilization efficiency of CaO_2 was decreased [21,24]. Consequently, the appropriate combination method of biochars and CaO_2 is the key to strengthening the oxygen release of CaO_2 and improving the utilization efficiency of the oxygen release agent (Lu et al., 2017; [53]).

It has been reported in the literature that the properties and structure of biochars will affect their loading and catalytic performance. Kumar et al. find nitrogen species in biochars will interact with RuO_x to enhance the electron density of Ru and improve the activity of the catalyst for selective (hetero) arene hydrogenation [22]. Yang et al. use CO_2 to treat biochars, which improves the specific surface area and pore volume, enabling them to enrich more amorphous Sn structures, and improving the yield and selectivity of fructose in terms of catalytic performance (Yang, X. et al., 2019). Luo et al. use $ZnCl_2$ to modify biochars and find that the increase of specific surface area improves the dispersion of Ni, while the increase of oxygen-containing functional groups introduces more active sites for catalytic reactions [29]. Therefore, the relationship between the properties of biochars and their functions is critical for a better application of the biochar materials. Unfortunately, the effects of biochar properties on the oxygen releasing performance of CaO_2 has not been reported previously.

Based on the above consideration, this investigation aims at developing an innovative biochar-loaded oxygen-releasing material for bioremediation of petroleum containment and establishing the relationship between the properties of the materials and the remediation performance. To this end, CaO_2 and biochars were incorporated using an in-situ precipitation method to enhance the oxygen release ability and increase the utilization efficiency of CaO_2. Biochars were obtained by pyrolysis and subsequent treatment of alkali activation or acid oxidation to regulate the pore structure and oxygen content. The physicochemical properties of the prepared biochars were characterized, and the CaO_2 loading amounts on the biochars were quantified. The oxygen release properties of the carbon-based materials were studied in a static environment, and the conversion efficiency of the oxygen-release materials was quantitatively evaluated. Finally, those materials were selected to apply in the biodegradation experiment to investigate their influence on the bioremediation efficiency. Accordingly, the relationship between the biochar properties, the oxygen releasing performance, and the remediation effects was established. The results of this study will lay an important foundation for promoting the application of carbon-based materials in the remediation of oil-contaminated groundwater.

2. Materials and methods

2.1. Materials

Bamboo powder was purchased from local bamboo processing enterprises. Potassium hydroxide (KOH), anhydrous calcium chloride ($CaCl_2$), ammonia ($NH_3{\cdot}H_2O$) and ammonium sulphate ($(NH_4)_2{\cdot}SO_4$) were purchased from Sinopharm Chemical Reagent Co., Ltd, China. Nitric acid (HNO_3), hydrogen peroxide solution (H_2O_2), potassium permanganate ($KMnO_4$), and sulfuric acid (H_2SO_4) were purchased from Nanjing Chemical Reagent Co., Ltd, China. Polyethylene glycol 200 (PEG 200) and manganese sulfate ($MnSO_4$) were obtained from Shanghai McLean Biochemical Technology Co., Ltd, China. All the chemicals used were of analytical grade. *Pseudomonas* sp. SB was obtained from the Key Laboratory of Soil Environment and Pollution

Remediation, Institute of Soil Science, Chinese Academy of Sciences. Diesel oil was purchased from local gas station.

2.2. Preparation of the oxygen-releasing materials

The raw bamboo powder (sawdust) was crushed and sieved to 100 mesh (0.15 mm), washed with deionized water, and dried at 80 ℃ overnight. The obtained biomass materials were pyrolyzed in a tube furnace under an N_2 atmosphere. The pyrolysis temperature was increased from 25 ℃ to a certain temperature (500 ℃ or 800 ℃) at a rate of 10 ℃·min^{-1} and then kept at the peak temperature for 2 h before starting to cool down. The obtained biochars were named BP-500 and BP-800, respectively.

To further reveal the relationship between the physicochemical properties of the biochars and the oxygen release performance, the obtained biochars were modified using chemical activation methods. KOH was used as the activation agent using an impregnation method. Briefly, 10 g of biochars were mixed into a solution of 50 mL ultrapure water with 20 g KOH and impregnated for 1 h. The slurry was dried at 105 ℃ overnight. The resultant mixture was heated and activated in a tube reactor at 800 ℃ under an N_2 atmosphere for 2 h. All the samples were washed to neutral pH and dried overnight to obtain BPAC-500 and BPAC-800. Then the activated biochars were further treated using a strong acid solution. In particular, the biochars were mixed with 7 M HNO_3 solution, and oxidized in a 60 ℃ oil bath for 12 h. The oxidization was conducted under magnetic stirring in a three-necked flask equipped with a reflux condenser [2,59]. The oxidized activated biochars were washed repeatedly with ultrapure water until the pH of the effluent water was constant, dried at 105 ℃ for 24 h, and stored in a desiccator for last use. The oxidized activated carbons were named BPOC-500, and BPOC-800, respectively.

The method of loading CaO_2 onto the above carbon materials was based on the literature report [1,26]. First, 2 g of prepared carbon materials were added to the $CaCl_2$ aqueous solution, which was prepared by dissolving 2 g of $CaCl_2$ in 20 mL of ultrapure water. After magnetic stirring for 1 h, 80 mL of PEG 200 and 15 mL of 1 M $NH_3{\cdot}H_2O$ were added to the above solution. Then 20 mL of 30% H_2O_2 solution was added dropwise to the mixture at the rate of 1 mL·min^{-1} using a syringe pump under vigorously stirring in an ice water bath Rastinfard [41]. The stir was kept for 2 h to ensure the complete reaction of the compounds.

After the mixing, 1 M $NH_3{\cdot}H_2O$ was added to adjust the pH of the solution to pH= 10, then the suspension was filtered. The solid was washed three times using cold ultrapure water and absolute ethanol respectively and then put into a vacuum drying oven at 60 ℃ for 12 h.

2.3. Characterization of the oxygen-releasing materials

The elemental composition of the biochars was measured using an element analyzer (Vario EL-III, Elementar, Germany). The pore structure properties of the biochar materials were characterized via a nitrogen adsorption-desorption device (BSD-PM, BeiShiDe, China). The surface functional groups of the samples were examined with FT-IR spectroscopy (VERTEX 80 V, Bruker, Germany) using KBr pellets in the wavenumber range of 400–4000 cm^{-1} at room temperature. The analysis of elements and valence states on solid surface was executed the X-ray photoelectron spectroscopy (XPS, Thermo Scientific K-Alpha) by using Al Kα radiation.

XRD was conducted to identify the crystallographic structure of CaO_2 on the surface of the samples using a computer-controlled X-ray diffractometer (Ultima IV, Rigaku, Japan). The changes in surface morphology were observed by a Cold Field Scanning electron microscope (Regulus 8100, Hitachi, Japan).

The CaO_2 content of the oxygen-releasing materials was evaluated using titration with $KMnO_4$ in acidic conditions Mosmeri, Shavandi [33]. Briefly, 100 mg of oxygen-releasing materials were added to 20 mL ultrapure water and fully stirred to disperse evenly. Then 10 mL of 2 M H_2SO_4 and 1 mL of 0.05 M $MnSO_4$ were added and stirred. After the full reaction, the solid materials were removed from the solution by filtration. The filtrate obtained was titrated with 0.02 mol·L^{-1} $KMnO_4$ standard solution. $KMnO_4$ titration principle was shown in the following formula.

$$CaO_2 + H_2SO_4 = CaSO_4 + H_2O_2$$

$$5H_2O_2 + 2KMnO_4 + 3H_2SO_4 = 5O_2 + 2MnSO_4 + 8H_2O + K_2SO_4$$

The calculation method of CaO_2 content in the oxygen releasing materials was shown as follows:

$$W_{CaO_2} = \frac{2.5C_{KMnO_4} \cdot V_{KMnO_4} \cdot M_{CaO_2}}{m}$$

Where W_{CaO_2} was the content of CaO_2 in the oxygen releasing materials, C_{KMnO_4} was the concentration of $KMnO_4$ (0.02 mol·L^{-1}), V_{KMnO_4} was the volume of $KMnO_4$ consumed, M_{CaO_2} was the relative molecular mass of CaO_2, and m was the mass of the corresponding oxygen releasing materials.

2.4. Oxygen release experiment

The oxygen release experiments were conducted in 1 L cylindrical organic glass reactors equipped with a sealing cap. First, 1 L of ultrapure water was added to the reactors. Then, sufficient N_2 was filled into the ultrapure water to reduce the DO concentration to lower than 0.1 mg·L^{-1}. Thirty milligrams of pure CaO_2 were added into the ultrapure water as the control group for the oxygen release experiments. The adding amount of the carbon-based materials was calculated according to their CaO_2 contents, to ensure that the added materials contain 30 mg of CaO_2. The DO content in the solution was measured using a DO meter (Multi 3620 IDS, WTW, Germany), and the data was automatically saved every 5 min. When DO content reached stable, it could be regarded as the end of oxygen release. After the reaction, the solution was filtered and the solid phase was titrated with $KMnO_4$ to explore the remaining CaO_2 content in the samples. All samples were tested in triplicate to ensure the accuracy of data.

2.5. Biodegradation experiment

The strain *Pseudomonas* sp. SB was cultured in the Luria Broth medium at 30 °C with shaking at 180 rpm for 48 h and harvested by centrifugation at 8000 rpm for 5 min at 4 °C. Cell pellet was washed twice with sterile water and re-suspended in sterile water to obtain a density of 10^8 colony-forming units (cfus) mL^{-1} [50].

The soil was dried and sieved to 10 mesh (0.25 mm). Thirty-three grams of soil, 100 mL of phosphate buffer solution (pH=6.848) and 100 mg of ammonium sulfate were added into glass bottles respectively and sterilized by autoclaving. The purpose of adding phosphate buffer solution was to reduce the effect of $Ca(OH)_2$ generated by CaO_2 on pH. Then 1 mL 0# diesel oil was added into each glass bottle. After measuring the initial pH and DO values of mixed solution, 1 mL bacterial suspension was added into each glass bottle. The six treatments set up in quadruplicate were: (1) Untreated control, without adding anything; (2) BP500; (3) BP800; (4) 100 mg CaO_2; (5) CaO_2 @BP500; (6) CaO_2 @BP800. The adding amount of CaO_2 @BP500 and CaO_2 @BP800 was calculated according to their CaO_2 contents, to ensure that the added materials contain 100 mg of CaO_2. The adding amount of BP500 and BP800 was calculated according to the content of biochar in CaO_2 @BP500 and CaO_2 @BP800, respectively. After adding the corresponding materials, glass bottles were sealed and put into the constant temperature shaker and oscillated at 30 ℃ and 180 rpm for 10 days.

2.6. DNA extraction and quantitative real-time PCR (qPCR)

For each sample, 0.50 mL of water soil mixture was used to extract microbial DNA using a FastDNA® Spin Kit (MP Biomedicals, Solon, OH) according to the manufacturer's protocols. The DNA concentrations and qualities were determined using a NanoDrop™ 1000 spectrophotometer (Thermo Fisher Scientific, Waltham, MA).

The 16 S rRNA gene abundance was determine by qPCR using primers 515 F 5′- GTGCCAGCMGCCGCGG-3′ and 907 R 5′-CCGTCAATTCMTTTRAGTTT-3′. All qPCR reactions process were performed following to Hou et al. [16]. The amplification efficiency was 112% with an R^2 value of 0.990.

2.7. Soil diesel oil extraction and analysis

The method of soil diesel oil extraction and analysis was referring to Hou et al. [15]. The freeze-dried soil sample was taken in 2 g and extracted using 70 mL dichloromethane by a Soxhlet extractor for 24 h. The extracts were rotary-evaporated and fully dissolved in 3 mL n-hexane. Then 2 mL hexane dissolved extract was taken to pass through chromatographic columns, which was composed of 1 g anhydrous sodium sulfate and 4 g florisil. Then 30 mL of n-hexane was used for elution and concentrate to 2 mL with N_2. The residual content of diesel oil in soil was determined by GC-FID. The recovery rates were 87–119%, and the detection limit of this method was 6 $mg{\cdot}kg^{-1}$.

3. Results and discussion

3.1. Characteristics of carbon materials

3.1.1. Elemental composition and surface pore structure analysis

Table 1 showed the elemental composition and surface pore structure data of the 6 kinds of carbon materials. From the table, it can be seen that the H content in biochars obtained at 800 ℃ was basically lower than that at 500 ℃. This is within expectation, since higher pyrolysis temperatures enhance the escape of volatile matter from biomass, as has been widely reported in the literature. The specific surface areas of biochars obtained by simple pyrolysis were relatively low, with the highest value of 292 $m^2{\cdot}g^{-1}$ measured for BP-800.

After KOH impregnation and activation, the O content in the biochar samples increased by 2.7–4.2%, which was due to the introduction of oxygen-containing functional groups on the sample surface during the reaction with KOH. The specific surface area of the corresponding activated carbons increased significantly, with BPAC-500 reaching the maximum of 1724 $m^2{\cdot}g^{-1}$. The average pore diameter of the pyrolysis chars was relatively large, while that of the activated carbons became smaller, indicating the obvious formation of micropores on the surface of the KOH-activated chars. The significant increase in the number of micropores contributes to the increases in the specific surface area Tan, Xu [43].

Table 1
Elemental composition and surface pore structure of the carbon materials.

Sample	Elements composition[a] (wt%)				Surface area ($m^2{\cdot}g^{-1}$)	Pore volume ($cm^3{\cdot}g^{-1}$)	Average pore size (nm)
	C	H	N	O			
BP-500	85.66	2.71	0.52	11.05	19.69	0.06	12.21
BPAC-500	83.00	1.18	0.34	15.28	1724.70	0.70	1.63
BPOC-500	76.54	2.21	0.48	20.77	1475.78	0.65	1.77
BP-800	86.06	0.88	0.65	12.39	291.52	0.12	1.58
BPAC-800	83.46	1.15	0.30	15.08	1250.91	0.51	1.65
BPOC-800	78.31	1.21	0.49	19.99	1171.98	0.54	1.83

[a] dry and ash-free basis

After HNO_3 oxidation, the O content of the activated chars further increased by about 5%, indicating that HNO_3 oxidation formed new oxygen-containing functional groups on carbon materials. Specifically, the strong oxidizing ability of HNO_3 could further oxidize the hydroxyl (-C-OH) and carbonyl (-C═O) functional groups to carboxyl functional groups (-COOH). After the oxidation of the activated chars, the average pore diameter increased slightly and the specific surface area decreased correspondingly to a certain extent, which should be caused by the erosion of HNO_3 on the samples and the wall collapse of some pores [59].

3.1.2. Surface functional groups analysis

The surface functional groups on different carbon materials were studied by FTIR analysis. It can be seen from Fig. 1 that the FTIR spectra of BP-500 contained a lot of weak peaks because it had not been completely pyrolyzed at 500 ℃ and many functional groups in biomass were retained. Except for BP-500, other samples showed similar FTIR spectra. The main peaks included the hydroxyl (-OH) peaks of phenol or alcohol at 3419 cm^{-1}, the C═C peak of aromatic components at 1617 cm^{-1}, and the C-O peak of polysaccharide acetal structures at 1113 cm^{-1}. The intensity of these peaks of the activated chars and the oxidized chars were stronger than that of pyrolyzed biochars at 800 ℃, indicating that KOH activation and HNO_3 oxidation introduced new oxygen-containing functional groups into the carbon materials. Specifically, the C═O peak belonging to the carboxyl (-COOH) appeared in the oxidized chars at 1704–1720 cm^{-1}, indicating that carboxyl groups were introduced due to the oxidation of HNO_3 Wu et al., [54]; Wu, Dai [55]. The hydroxyl (- OH) peaks at 3419 cm^{-1} also became stronger in activated carbon and oxidized carbon. The increase of these oxygen-containing functional groups is beneficial to the loading of oxygen releasing agent CaO_2.

3.1.3. Surface elements and valence states analysis

Fig. 2 showed the fitting of C 1 s spectrum. The peaks at 284.8, 286.4 and 288.4 eV can be fitted by the C 1 s X-ray photoelectron spectroscopy. These peaks may come from C-C, C-O and C═O, respectively [56]. The C-C peak of BP-800 was sharper than that of BP-500, indicating that the degree of aromatization in carbon materials increased with the increase of pyrolysis temperature. The peak areas of C-O and C═O gradually increase after activation and oxidation, indicating that KOH activation and HNO_3 oxidation increase the oxygen-containing functional groups in carbon materials [7,12]. This was consistent with the conclusion of element analysis and FTIR.

Fig. 3 showed the fitting of O 1 s spectrum. The peaks at 531.6 eV belongs to ketone, carbonyl or lactone group, the peaks at 532.6 eV belongs to ether and alcohol, and the peaks at 535.5 eV belongs to carboxyl group Ding [11]. By comparing the change of O 1 s peaks

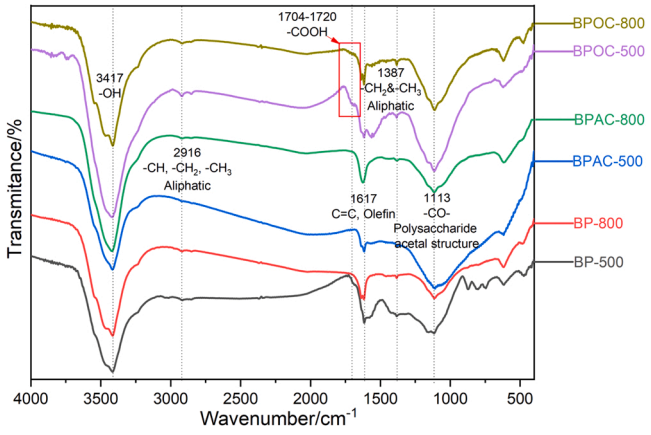

Fig. 1. FTIR transmission spectra of bamboo powder carbon materials.

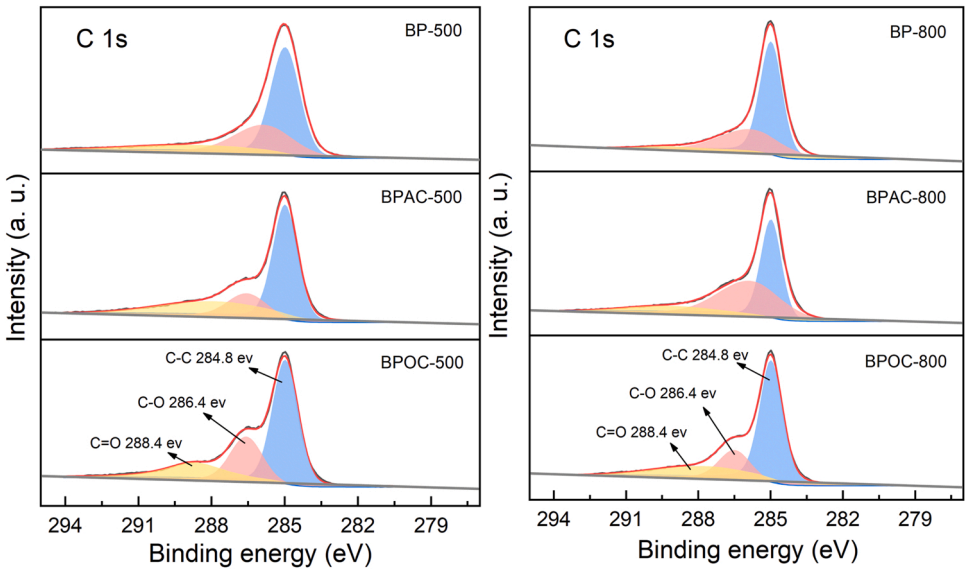

Fig. 2. XPS C 1 s spectra of bamboo powder carbon materials.

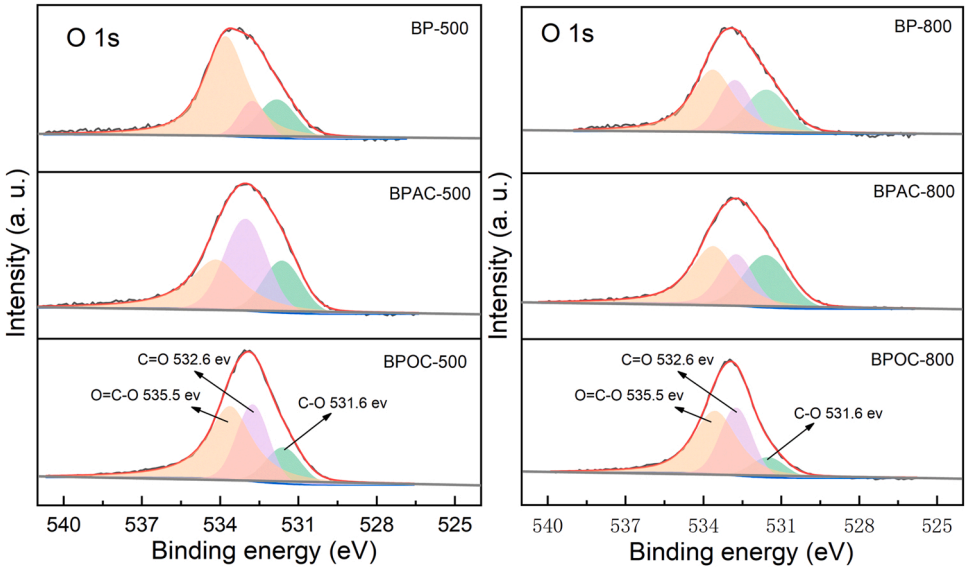

Fig. 3. XPS O 1 s spectra of bamboo powder carbon materials.

spectrum among pyrolyzed chars, activated chars and the oxidized chars, it can be seen that after HNO_3 oxidation, the content of C-O bond decreased, while that of C═O bond and O═C-O bond increased. The oxygen-containing functional groups were negatively charged during deprotonation, so the activated and oxidized carbon materials have stronger ability to load CaO_2 Tan, Hong [44].

3.2. Characteristics of oxygen-releasing materials

3.2.1. Crystal shape analysis

Fig. 4 shows the XRD patterns of the different oxygen-releasing materials prepared with bamboo powder chars. As shown, all the samples had a strong wide peak at $2\theta = 23.8°$ and a weak wide peak at $2\theta = 43.8°$, corresponding to (100) and (002) crystal planes of carbon materials respectively. Compared with the PDF card library, it can be found that the phase and intensity of the other main peaks were consistent with the PDF card of CaO_2 (JCPDS Card No. 03–0865), which contained four major peaks at $2\theta = 30.2°$, 35.6°, 47.3°and 53.2°. This indicated that CaO_2 was successfully synthesized and loaded on carbon materials. Besides, there was a weak peak at $2\theta = 29.4°$, which corresponds to the (104) crystal plane of $CaCO_3$ (JCPDS Card No. 05–0586). The formation of $CaCO_3$ may be due to the reaction of Ca^{2+} with CO_2 in the air under alkaline conditions during the preparation process Kaewdee, Rujijanagul [18]. By comparing the intensity of CaO_2 peaks and carbon materials, the relative amount of CaO_2 in the samples can be roughly obtained. The highest content of CaO_2 was found in CaO_2 @BPOC-500, which might be related to its highest O content. In addition, peaks of SiO_2 at $2\theta = 26.6°$ were observed in the oxygen-releasing materials prepared using pyrolyzed char, which may be due to the relatively high ash content in the biomass feedstock.

3.2.2. Microtopography analysis

Fig. 5(a) (b) displayed the surface morphology and EDS scanning diagram of CaO_2 @BP-500 at 3000 times. It can be seen from Fig. 5(a) that the surface of the carbon-based materials was flat and smooth, and some small particles were attached tightly to the biochars. According to

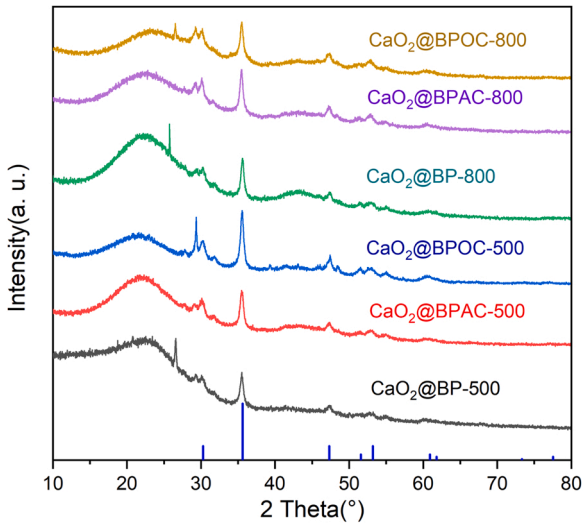

Fig. 4. XRD patterns of carbon-based oxygen releasing materials.

the EDS scanning image shown in Fig. 5(b), these particles contained a large amount of Ca^{2+}, and the mass fraction of Ca^{2+} reached 5.98 wt%, indicating that CaO_2 particles had been successfully loaded on the biochars surface.

Fig. 5(c) (d) showed the surface morphology of CaO_2 @BP-500 at 50000 times. Fig. 3(c) exhibited that some of the CaO_2 particles had embedded into the macropores of the biochars. It can be reasonably speculated that the macropore structure of the carbon material can protect CaO_2, and thus could potentially prolong the oxygen release period. Fig. 3(d) showed that some nanoparticles of CaO_2 were agglomerated to large particles. The average size of these nanoparticles was about 10 nm, which agreed with the conclusion reported in the literature [35]; Wu, B. et al., 2017), thus they can enter the pores greater than 10 nm on the surface of the biochars.

3.3. CaO_2 loading capacity and oxygen release ability

Fig. 6 showed the oxygen release potentials of all the biochar-based materials, including CaO_2 contents on the biochar materials, oxygen release time, and the final DO concentration in the water. Basically, the loading amounts of CaO_2 conformed with the order of oxidized char > activated char > pyrolyzed char. This was consistent with the results of XRD analysis, which indicated a similar trend of relative peak heights of CaO_2 (Fig. 4). For the pyrolytic chars at different temperatures, although the pore structures were significantly different, the loading amounts of CaO_2 were relatively close. This indicates that the loading capacity of the biochars may be poorly related to the pore structure of the biochars. The loading amount of CaO_2 on CaO_2 @BP-500 was 6.17 wt%, which was quite close to the EDS scanning result (5.98 wt%). Activation of the biochars using KOH dramatically increased both the oxygen content and the specific surface area of the biochars, while obviously decreasing the average pore size of pyrolytic biochars, resulting in the noticeable increments in CaO_2 loading capacities of BPAC-500 and BPAC-800. Further oxidizing the activated biochars exhibited a clear rise in the oxygen contents but a minor effect on the structure properties. Correspondingly, the CaO_2 loading amounts on the oxidized biochars increased remarkably, proving that the loading capacity of the biochars was determined by their oxygen contents. HNO_3 oxidation created new oxygen-containing functional groups on the surface of carbon materials, especially carbonyl and carboxyl groups. These oxygen-containing functional groups can form Ca-O with Ca^{2+}, which enhanced the loading capacity for CaO_2 [9,31].

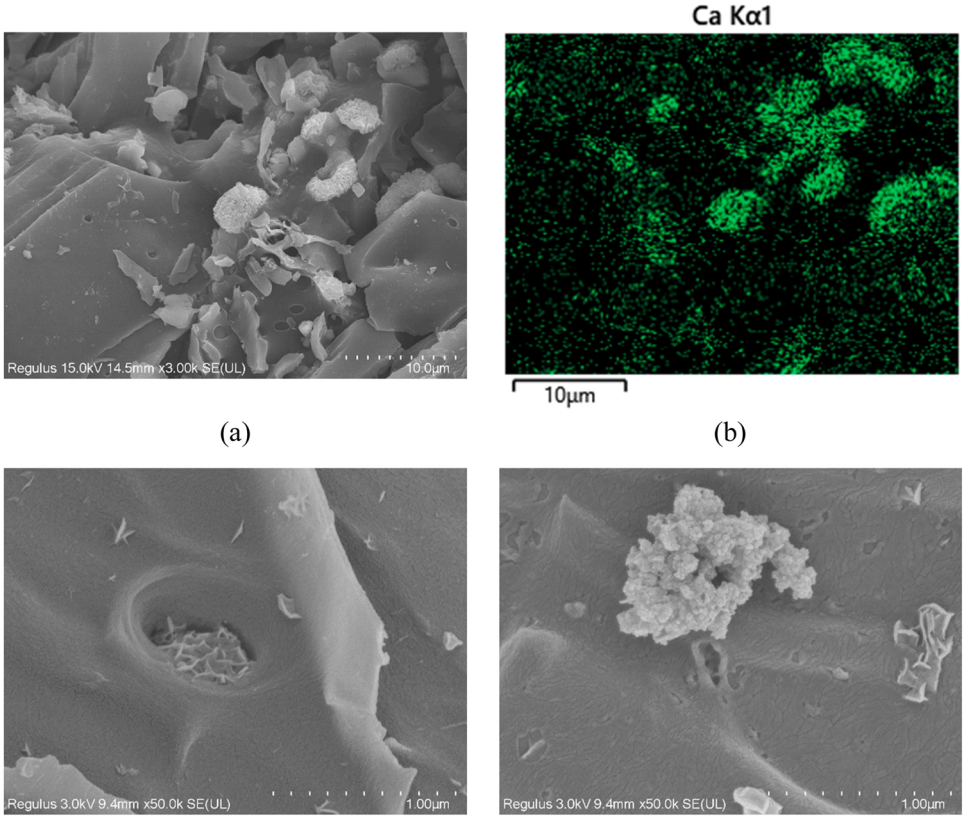

Fig. 5. SEM and EDS scanning of CaO_2 @BP-500 at (a) (b) 3000 times and (c) (d) 50000 times.

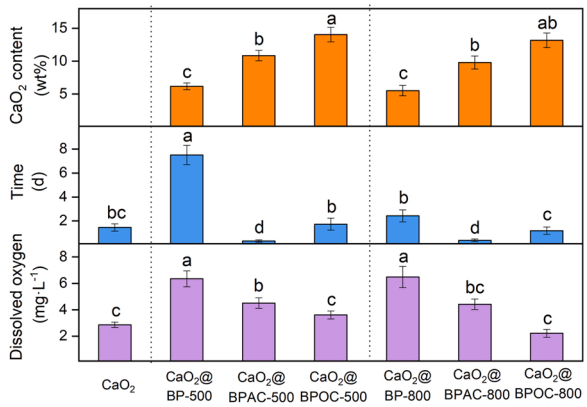

Fig. 6. CaO_2 content, oxygen release time and amount of pure CaO_2 and bamboo powder carbon-based oxygen releasing materials.

Fig. 6 also displayed the oxygen release periods of the biochar-based materials. For pure CaO_2 without loading, the oxygen release time was only 1.5 days, which was relatively short, and similar to the pure CaO_2 in other literatures [14,32]. Interestingly, although the CaO_2 loading amount of CaO_2 @BP-500 was relatively low, the oxygen release lasted as long as 7.5 days, representing the longest release period. It should be noted that among all the biochars, BP-500 exhibited the largest average pore diameter of ~12 nm. Considering that the size of the synthetic CaO_2 particles was about 10 nm (shown in Fig. 5(d)), the nanoparticles were able to enter many of the pores of BP-500. Therefore, the appropriate pore size of BP-500 showed a great potential to protect CaO_2 and hinder its contact with water and thus prolonging the oxygen release period. Although the CaO_2 loading amount of CaO_2 @BP-800 was close to that of CaO_2 @BP-500, the oxygen release time was significantly reduced to 2.4 days. This may be related to the reduced pore size of BP-800 biochar, which proves again the importance of suitable pore size during the oxygen release process. For the KOH-activated materials, namely CaO_2 @BPAC-500 and CaO_2 @BPAC-800, their oxygen release periods were considerably shortened to less than 0.4 days. The reason may be that after the activation, the pore structure of carbon materials was immoderately developed and dominated by micropores so that most CaO_2 nanoparticles can hardly enter the pores. Meanwhile, the increased oxygen content in the biochars promoted the adsorption of CaO_2 on the surface. As a result, more CaO_2 nanoparticles are exposed on the surface of the biochars and will release oxygen rapidly upon contact with water. In addition, the increment in the oxygen content of oxidized biochars (BPOC-500 and BPOC-800) induced a slight increase in the oxygen release periods to 1.2–1.7 days, implying that the oxygenated functional groups on the surface of biochars also demonstrated a weak effect on the oxygen release period. All oxygen-releasing materials were collected for $KMnO_4$ titration after the oxygen release experiments. The titration results showed that there was no residual CaO_2 in them, indicating that CaO_2 was completely reacted in the oxygen release experiments. However, there were some residues in the pure CaO_2 group, which might be caused by the agglomeration of CaO_2 and the formation of insoluble $Ca(OH)_2$ on the surface. This result confirms the complete conversion of the oxygen release material, which is favorable for reducing the cost of the remediation technology.

The DO concentration in the water was also strongly affected by the biochar properties. As shown in Fig. 6, the DO content for pure CaO_2 was 2.9 $mg{\cdot}L^{-1}$, which was close to the optimized DO concentration (3 $mg{\cdot}L^{-1}$) for the growth of microbials (Gholami et al., 2018). CaO_2 @BP-500 and CaO_2 @BP-800 presented the highest DO concentration of 6.4–6.5 $mg{\cdot}L^{-1}$, although the pore structures of the biochars support were noticeably different. Loading CaO_2 on the activated biochars (CaO_2 @BPAC-500 and CaO_2 @BPAC-800) obviously decreased the DO concentration to about 4.5 $mg{\cdot}L^{-1}$. Oxidation of the activated biochars using HNO_3 (CaO_2 @BPOC-500 and CaO_2 @BPOC-800) further reduced the DO concentration to 3.6 $mg{\cdot}L^{-1}$ and 2.2 $mg{\cdot}L^{-1}$, respectively. It was interesting to find that the higher the oxygen content in biochars, the lower the DO concentration. Previous studies have revealed two main pathways for the reaction of CaO_2 with water, one is to decompose into O_2 and $Ca(OH)_2$, and the other is to produce H_2O_2 and $Ca(OH)_2$. These two pathways compete with each other, therefore if more CaO_2 is converted into H_2O_2, less O_2 can be generated [51]. Correspondingly, we speculated that the activated biochars and the oxidized biochars might have promoted the decomposition of CaO_2 to produce more H_2O_2. As a result, the DO concentration was lowered. Moreover, the persistent free radicals (PFRs) on biochars may also play an important role in reducing the DO releasing amount. It has been reported in the literature that PFRs on biochar materials displayed a positive catalytic effect on the decomposition of CaO_2 to generate hydroxyl free radicals (·OH) [30,63]. The introduction of K^+ and the increase of O content after KOH activation increase the content of PFRs, resulting in the enhancement of catalytic activity. Meanwhile, the increased specific surface area of the activated biochars gives extra rise to the catalytic active sites. After HNO_3 oxidation, the PFRs content in biochars is further increased along with the increase of O content so that the DO concentrations of both CaO_2 @BPOC-500 and CaO_2 @BPOC-800 reached the minimum.

From the above discussion, the influence of biochars properties on the oxygen release performance of CaO_2 is mainly reflected in two aspects. On the one hand, the CaO_2 loading capacity of different biochars is mainly affected by the O content of biochars. On the other hand, even with the equivalent dosage of CaO_2, the oxygen release periods and DO concentration are significantly different when different biochars are used as carriers, indicating that the properties of biochars exhibit an important impact on the oxygen release performance of CaO_2. Among them, the periods of oxygen release are mainly affected by the pore structure, while the concentration of DO is principally controlled by the content of O. Hence, the preparation of biochars with appropriate pore structure and O content is critical to optimizing the oxygen release performance of CaO_2.

3.4. Biodegradation experiment

The initial DO concentration and pH values of the mixed solution were and 7.5 $mg{\cdot}L^{-1}$ and 6.9, respectively. After the 10 days biodegradation experiment, the DO concentrations after biodegradation were lower than 0.5 $mg{\cdot}L^{-1}$ in all the groups, indicating that the oxygen has been completely consumed, which was majorly due to the relatively low CaO_2 dosage and rapid consuming by the bacterial inoculation. The final pH value of the groups with different treatments was shown in Fig. 7. As shown, the final pH values of most groups (with or without oxygen-releasing materials) changed slightly from the initial value of 6.9–6.6–6.7, except those adding CaO_2 and CaO_2 @BP500. The latter two groups exhibited marginally lower pH values of below 6.3, which may be due to the fact that the degradation process of the two experimental groups was mainly aerobic degradation, and thus more acidic

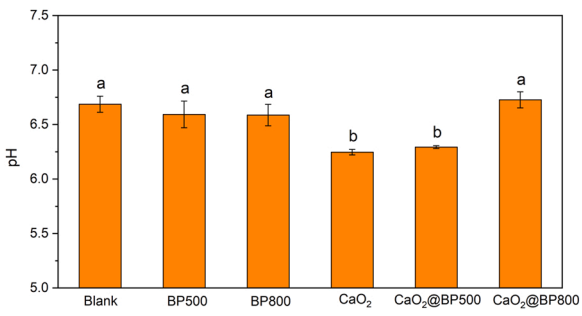

Fig. 7. pH value in different treatments at the end of the biodegradation experiments.

substances were produced. The diesel oil used in this experiment is 0# diesel oil, which contains about 68% alkanes. Compared with naphthenes and aromatics, alkanes are more biodegradable. Alkanes are commonly degraded by mono-terminal oxidation. Terminal methyl is usually oxidized to primary alcohols and then converted to aldehydes and carboxylic acids, which tend to decrease the pH of the solution [37, 45].

Fig. 8 and Fig. 9 showed the 16 S rRNA gene copy numbers and diesel oil degradation rates of different treatment groups at the end of the experiment, respectively. The amounts of 16 S rRNA copy numbers can reflect the relative abundance of degrading bacteria in the experimental groups Vetrovsky [46]. It can be seen from Fig. 8 that the untreated blank group had the lowest 16 S rRNA gene copy number, which was within expectations. The 16 S rRNA gene copy number in the group added with CaO_2 @BP800 was almost twice that of other groups. According to Fig. 4, the possible reason was that the material CaO_2 @BP800 had a short oxygen release cycle and strong oxygen release ability, which led to the material releasing a large amount of oxygen in the early stage of the experiment. The degrading bacteria of the group multiplied in large numbers in the early stage of the experiment with sufficient oxygen and nutrients, leading to the highest 16 S rRNA gene copy number. This also showed the importance of complete conversion of CaO_2 in biochar-based materials.

According to Fig. 9, the blank group with the least number of degrading bacteria has the lowest diesel oil removal. The diesel oil removal of the groups adding BP500 and BP800 was slightly higher than that of the blank group, which may be due to the physical adsorption of diesel oil by biochars. Attributed to aerobic degradation, the diesel oil removal rate of the groups adding CaO_2 and CaO_2 @BP500 was about 4–10% higher than that in the groups adding BP500 and BP800. Comparing with the blank group (with microorganisms only), these groups showed negligible changes in the removal rate of diesel oil. This indicates that the removal of contaminants is not strongly related to the oxidation of calcium peroxide and the electron transport function of biochar. On the other hand, in the blank group with only microorganisms, the remediation efficiency reached about 32%, indicating that the main removal effect in the biodegradation test was contributed by *Pseudomonas* sp. SB. The highest removal of diesel oil was achieved in the CaO_2 @BP800 group, which was about 10% higher than the pure CaO_2 group. It is indicated that an obvious enhancement in the diesel oil removal efficiency could be obtained by applying the CaO_2 @BP800 material. The highest content of degrading bacteria (shown in Fig. 8) in this group may contribute the most to the highest remediation performance.

4. Conclusions

Concisely, biochars were used as carriers to improve the oxygen releasing performance of CaO_2. Results implied that biochar properties could be regulated using base/acid treatment and would further determine the CaO_2 loading capacity and oxygen release performance. Biochars significantly increased the oxygen release time and amount of CaO_2 to up to 5 times and 2 times, respectively, and a full conversion of CaO_2 was observed for the biochar-loaded materials. The relationship between the biochars properties and the oxygen release ability was consolidated. The biodegradation experiments of diesel oil using the prepared materials exhibited a final pH range of 6.25–6.73, and all the experimental groups attained a complete consumption of dissolved oxygen. The highest removal ratio of diesel oil was observed for CaO_2 @BC800, due to the maximized amount of bacteria. Therefore, biochar-based CaO_2 represents a promising oxygen-releasing material for bioremediation of petroleum-contaminated groundwater.

CRediT authorship contribution statement

Chen Shen: Conceptualization, Visualization, Investigation, Writing – original draft, **Gang Wu**: Methodology, Data curation, **Jun Sun**: Visualization, Investigation, **Jinyu Hou**: Conceptualization, Funding acquisition, **Hongqi Sun**: Investigation, Resources, **Kuan Ding**: Conceptualization, Supervision, Writing – review & editing, Funding acquisition, **Wuxing Liu**: Supervision, Project administration, **Shu Zhang**: Supervision, Funding acquisition.

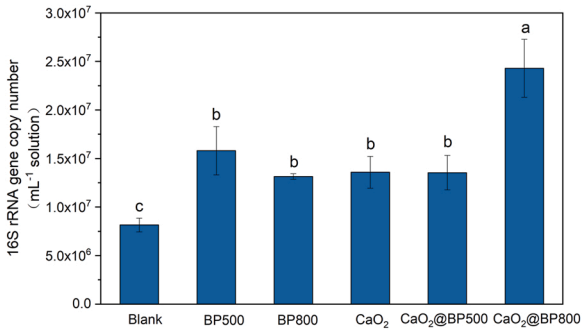

Fig. 8. . 16 S rRNA gene copy numbers in different treatments at the end of the biodegradation experiments.

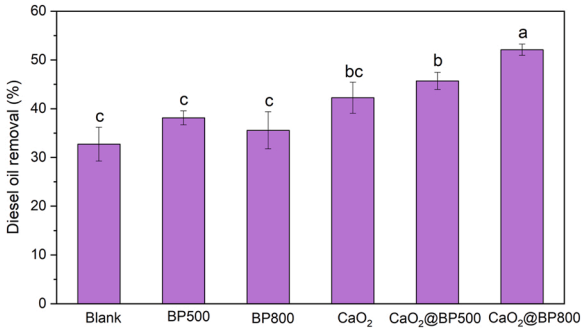

Fig. 9. Diesel oil removal in different treatments at the end of the biodegradation experiments.

Declaration of Competing Interest

The authors declare that they have no known competing financial interests or personal relationships that could have appeared to influence the work reported in this paper.

Data availability

Data will be made available on request.

Acknowledgements

This study is supported by the Ministry of Science and Technology of China (2018YFE0183600), the National Nature Science Foundation of China (52106251), the National Key Research and Development Program of China (2021YFC1808903), and the Natural Science Foundation of Jiangsu Province (BK20200792).

References

[1] Farooq Ali, Sun Lyu, Ahmad Li, Abbas Shan, Synthesis of controlled release calcium peroxide nanoparticles (CR-nCPs): characterizations, H_2O_2 liberate performances and pollutant degradation efficiency, Sep. Purif. Technol. (2020) 241, https://doi.org/10.1016/j.seppur.2020.116729.

[2] Vivekanandhan Anstey, Misra, Mohanty Rodriguez-Uribe, Oxidative acid treatment and characterization of new biocarbon from sustainable Miscanthus biomass, Sci. Total Environ. 550 (2016) 241–247, https://doi.org/10.1016/j.scitotenv.2016.01.015.

[3] Kaszycki Brzeszcz, Aerobic bacteria degrading both n-alkanes and aromatic hydrocarbons: an undervalued strategy for metabolic diversity and flexibility, Biodegradation 29 (4) (2018) 359–407, https://doi.org/10.1007/s10532-018-9837-x.

[4] Sun Bu, Liu Ma, Pan, Wei Gong, Shallow Groundwater Quality and Its Controlling Factors in the Su-Xi-Chang Region, Eastern China, Int J. Environ. Res Public Health 17 (4) (2020), https://doi.org/10.3390/ijerph17041267.

[5] Wu Chang, Lin Wang, Fabrication of novel rhamnolipid-oxygen-releasing beads for bioremediation of groundwater containing high concentrations of BTEX, Int. Biodeterior. Biodegrad. 116 (2017) 58–63, https://doi.org/10.1016/j.ibiod.2016.10.001.

[6] Gao Chen, Fang Li, Bhatnagar Bolan, Hou Gao, Song Wang, Shaheen Yang, Chen Meng, Wang Rinklebe, Engineered biochar for environmental decontamination in aquatic and soil systems: a review, Carbon Res. 1 (1) (2022) 4, https://doi.org/10.1007/s44246-022-00005-5.

[7] Yang Chen, Lin Liu, Zhang Wang, Li, Zhang Li, KOH modification effectively enhances the Cd and Pb adsorption performance of N-enriched biochar derived from waste chicken feathers, Waste Manag 130 (2021) 82–92, https://doi.org/10.1016/j.wasman.2021.05.015.

[8] Tatangelo Daghio, Gandolfi Franzetti, Careghini Papacchini, Saponaro, Bestetti Sezenna, Hydrocarbon degrading microbial communities in bench scale aerobic biobarriers for gasoline contaminated groundwater treatment, Chemosphere 130 (2015) 34–39, https://doi.org/10.1016/j.chemosphere.2015.02.022.

[9] Zhang Deng, Ye Zheng, Lin Niu, Zhou Fu, Adsorption recovery of phosphate from waste streams by Ca/Mg-biochar synthesis from marble waste, calcium-rich sepiolite and bagasse, J. Clean. Prod. (2021) 288, https://doi.org/10.1016/j.jclepro.2020.125638.

[10] Khudur Dike, Rani Hakeem, Surapaneni Shahsavari, Ball Shah, Biosolids-derived biochar enhances the bioremediation of diesel-contaminated soil, J. Environ. Chem. Eng. 10 (6) (2022), https://doi.org/10.1016/j.jece.2022.108633.

[11] Liu Ding, Adsorption of CO_2 from flue gas by novel seaweed-based KOH-activated porous biochars, Fuel (2020) 260, https://doi.org/10.1016/j.fuel.2019.116382.

[12] Choi Dissanayake, Yang Igalavithana, Wang Tsang, Lee, Ok Kua, Sustainable gasification biochar as a high efficiency adsorbent for CO_2 capture: a facile method to designer biochar fabrication, Renew. Sustain. Energy Rev. (2020) 124, https://doi.org/10.1016/j.rser.2020.109785.

[13] Chen, Hung Dong, Synthesis of magnetic biochar from bamboo biomass to activate persulfate for the removal of polycyclic aromatic hydrocarbons in marine sediments, Bioresour. Technol. 245 (Pt A) (2017) 188–195, https://doi.org/10.1016/j.biortech.2017.08.204.

[14] Shavandi Gholami, Amoozegar Dastgheib, Naphthalene remediation form groundwater by calcium peroxide (CaO_2) nanoparticles in permeable reactive barrier (PRB), Chemosphere 212 (2018) 105–113, https://doi.org/10.1016/j.chemosphere.2018.08.056.

[15] Liu Hou, Wang Wang, Franks Luo, PGPR enhanced phytoremediation of petroleum contaminated soil and rhizosphere microbial community response, Chemosphere 138 (2015) 592–598, https://doi.org/10.1016/j.chemosphere.2015.07.025.

[16] Liu Hou, Hu Wu, Luo, Christie Ma, Modulation of the efficiency of trace metal phytoremediation by Sedum plumbizincicola by microbial community structure and function, Plant Soil 421 (1–2) (2017) 285–299, https://doi.org/10.1007/s11104-017-3466-8.

[17] Gedalanga Jasmann, Mahendra, Blotevogel Borch, Synergistic Treatment of Mixed 1,4-Dioxane and Chlorinated Solvent Contaminations by Coupling Electrochemical Oxidation with Aerobic Biodegradation, Environ. Sci. Technol. 51 (21) (2017) 12619–12629, https://doi.org/10.1021/acs.est.7b03134.

[18] Chandet Kaewdee, Randorn Rujijanagul, Multicatalytic properties of nanoparticle CaO_2 synthesized by a novel, simple and economical method for wastewater treatment, Catal. Commun. 84 (2016) 151–154, https://doi.org/10.1016/j.catcom.2016.06.031.

[19] Meesala Kandanelli, Raju Kumar, Gandham, Kumar Peddy, Cost effective and practically viable oil spillage mitigation: Comprehensive study with biochar, Mar. Pollut. Bull. 128 (2018) 32–40, https://doi.org/10.1016/j.marpolbul.2018.01.010.

[20] Husain, Hejazi Khan, An overview and analysis of site remediation technologies, J. Environ. Manag. 71 (2) (2004) 95–122, https://doi.org/10.1016/j.jenvman.2004.02.003.

[21] Banejad Khodaveisi, Olyaie Afkhami, Dashti Lashgari, Synthesis of calcium peroxide nanoparticles as an innovative reagent for in situ chemical oxidation, J. Hazard Mater. 192 (3) (2011) 1437–1440, https://doi.org/10.1016/j.jhazmat.2011.06.060.

[22] Goyal Kumar, Singh Sarki, Bhaskar Ray, Narani, Natte Bordoloi, Biocarbon supported nanoscale ruthenium oxide-based catalyst for clean hydrogenation of arenes and heteroarenes, ACS Sustain. Chem. Eng. 8 (41) (2020) 15740–15754, https://doi.org/10.1021/acssuschemeng.0c05773.

[23] Erdeine Kis Laczi, Bounedjoum Szilagyi, Vincze Bodor, Rakhely, Perei Kovacs, New frontiers of anaerobic hydrocarbon biodegradation in the multi-omics era, Front Microbiol 11 (2020), 590049, https://doi.org/10.3389/fmicb.2020.590049.

[24] Jiang Li, Ruan, Miao Liu, Restoration of river sediment by calcium peroxide(CaO_2) combined with biochar, Huan jing ke xue= Huanjing kexue 41 (8) (2020) 3629–3636, https://doi.org/10.13227/j.hjkx.201912207.

[25] Luo Li, Song Zhang, Jiang, Zhang Cai, Autochthonous bioaugmentation-modified bacterial diversity of phenanthrene degraders in PAH-contaminated wastewater as revealed by DNA-stable isotope probing, Environ. Sci. Technol. 52 (5) (2018) 2934–2944, https://doi.org/10.1021/acs.est.7b05646.

[26] Xie Li, Wang Jiang, Tang Hu, Wu Luo, Enhanced phosphate removal from aqueous solution using resourceable nano-CaO_2/BC composite: Behaviors and mechanisms, Sci. Total Environ. 709 (2020), 136123, https://doi.org/10.1016/j.scitotenv.2019.136123.

[27] Zeng Liu, Wang Zhong, Cheng Liu, Yang, Liu Liu, Effect of rhamnolipid solubilization on hexadecane bioavailability: enhancement or reduction, J. Hazard Mater. 322(Pt B) (2017) 394–401, https://doi.org/10.1016/j.jhazmat.2016.10.025.

[28] Zhang, Xue Lu, Application of calcium peroxide in water and soil treatment: a review, J. Hazard Mater. 337 (2017) 163–177, https://doi.org/10.1016/j.jhazmat.2017.04.064.

[29] Dong Luo, Zhang Zhang, Song, Zhou Wang, Catalytic Activity and Reusability of Nickel-Based Catalysts with Different Biochar Supports during Copyrolysis of Biomass and Plastic, ACS Sustain. Chem. Eng. 10 (30) (2022) 9933–9945, https://doi.org/10.1021/acssuschemeng.2c02392.

[30] Yang Luo, Wang Pang, Lei, Huang Li, Unveiling the mechanism of biochar-activated hydrogen peroxide on the degradation of ciprofloxacin, Chem. Eng. J. 374 (2019) 520–530, https://doi.org/10.1016/j.cej.2019.05.204.

[31] Karnjanakom Maneechakr, Environmental surface chemistries and adsorption behaviors of metal cations (Fe^{3+}, Fe^{2+}, Ca^{2+} and Zn^{2+}) on manganese dioxide-modified green biochar, RSC Adv. 9 (42) (2019) 24074–24086, https://doi.org/10.1039/c9ra03112j.

[32] Beazley McCormac, Fabrication and characterization of biodegradable oxygen-releasing micromaterials for treatment of hypoxic environmental waters, J. Environ. Chem. Eng. 8 (4) (2020), https://doi.org/10.1016/j.jece.2020.103979.

[33] Alaie Mosmeri, Dastgheib, Tasharrofi Shavandi, Benzene-contaminated groundwater remediation using calcium peroxide nanoparticles: synthesis and process optimization, Environ. Monit. Assess. 189 (9) (2017) 452, https://doi.org/10.1007/s10661-017-6157-2.

[34] Hou O'Connor, Song Ok, Li, Tack Sarmah, Sustainable in situ remediation of recalcitrant organic pollutants in groundwater with controlled release materials: A review, J. Control Release 283 (2018) 200–213, https://doi.org/10.1016/j.jconrel.2018.06.007.

[35] Banejad Olyaie, Rahmani, Khodaveisi Afkhami, Development of a cost-effective technique to remove the arsenic contamination from aqueous solutions by calcium peroxide nanoparticles, Sep. Purif. Technol. 95 (2012) 10–15, https://doi.org/10.1016/j.seppur.2012.04.021.

[36] Shi Pan, Kuang Chen, Lu, Riaz Ullah, An investigation into biochar, acid-modified biochar, and wood vinegar on the remediation of saline−alkali soil and the growth of strawberries, Front. Environ. Sci. (2022) 10, https://doi.org/10.3389/fenvs.2022.1057384.

[37] Kim Park, Lee Kim, Kang Kim, Enhanced biodegradation of hydrocarbons by Pseudomonas aeruginosa-encapsulated alginate/gellan gum microbeads, J. Hazard Mater. 406 (2021), 124752, https://doi.org/10.1016/j.jhazmat.2020.124752.

[38] Wild Piatka, Kaule Hartmann, Gilfedder Kaule, Geist Peiffer, Barth Beierkuhnlein, Transfer and transformations of oxygen in rivers as catchment reflectors of continental landscapes: A review, Earth-Sci. Rev. (2021) 220, https://doi.org/10.1016/j.earscirev.2021.103729.

[39] Lee Rai, Kwon Kailasa, Ok, Kim Tsang, A critical review of ferrate(VI)-based remediation of soil and groundwater, Environ. Res 160 (2018) 420–448, https://doi.org/10.1016/j.envres.2017.10.016.

[40] Chen Rajapaksha, Zhang Tsang, Mandal Vithanage, Bolan, Ok Gao, Engineered/designer biochar for contaminant removal/immobilization from soil and water: Potential and implication of biochar modification, Chemosphere 148 (2016) 276–291, https://doi.org/10.1016/j.chemosphere.2016.01.043.

[41] Nazarpak, Moztarzadeh Rastinfard, Controlled chemical synthesis of CaO_2 particles coated with polyethylene glycol: characterization of crystallite size and oxygen release kinetics, RSC Adv. 8 (1) (2018) 91–101, https://doi.org/10.1039/c7ra08758f.

[42] De. Angelis, Jacobo Russo, Adsorption with catalytic oxidation in a recirculating bed reactor for contaminated groundwater, J. Water Process Eng. 23 (2018) 129–133, https://doi.org/10.1016/j.jwpe.2018.03.009.

[43] Sun Tan, Wang, Xu Xu, Sorption of mercury (II) and atrazine by biochar, modified biochars and biochar based activated carbon in aqueous solution, Bioresour. Technol. 211 (2016) 727–735, https://doi.org/10.1016/j.biortech.2016.03.147.

[44] Yuan Tan, Zhang, Huang Hong, Mechanism of negative surface charge formation on biochar and its effect on the fixation of soil Cd, J. Hazard Mater. 384 (2020), 121370, https://doi.org/10.1016/j.jhazmat.2019.121370.

[45] Varjani, Microbial degradation of petroleum hydrocarbons, Bioresour. Technol. 223 (2017) 277–286, https://doi.org/10.1016/j.biortech.2016.10.037.

[46] Baldrian Vetrovsky, The variability of the 16S rRNA gene in bacterial genomes and its consequences for bacterial community analyses, PLoS One 8 (2) (2013), e57923, https://doi.org/10.1371/journal.pone.0057923.

[47] Ma Wang, Chen Sun, Wang Zhang, Zhang Wang, Adsorption of enrofloxacin on acid/alkali-modified corn stalk biochar, Spectrosc. Lett. 52 (7) (2019) 367–375, https://doi.org/10.1080/00387010.2019.1648296.

[48] Miao Wang, Yang, Zhang Saleem, Enhanced adsorptive removal of carbendazim from water by FeCl3-modified corn straw biochar as compared with pristine, HCl and NaOH modification, J. Environ. Chem. Eng. 10 (1) (2022), https://doi.org/10.1016/j.jece.2021.107024.

[49] Wang Wang, Preparation, modification and environmental application of biochar: A review, J. Clean. Prod. 227 (2019) 1002–1022, https://doi.org/10.1016/j.jclepro.2019.04.282.

[50] Wang Wang, Liu Liu, Teng Hou, Christie Luo, Biosurfactant-producing microorganism Pseudomonas sp. SB assists the phytoremediation of DDT-contaminated soil by two grass species, Chemosphere 182 (2017) 137–142, https://doi.org/10.1016/j.chemosphere.2017.04.123.

[51] Zhao Wang, Chen Li, Qin Wang, Properties of calcium peroxide for release of hydrogen peroxide and oxygen: A kinetics study, Chem. Eng. J. 303 (2016) 450–457, https://doi.org/10.1016/j.cej.2016.05.123.
[52] Erto Wjihi, Ben Lamine Knani, Investigation of adsorption process of benzene and toluene on activated carbon by means of grand canonical ensemble, J. Mol. Liq. 238 (2017) 402–410, https://doi.org/10.1016/j.molliq.2017.04.021.
[53] Chang, Lin Wu, Improvement of Oxygen Release from Calcium Peroxide-polyvinyl Alcohol Beads by Adding Low-cost Bamboo Biochar and Its Application in Bioremediation, CLEAN - Soil, Air, Water 43 (2) (2015) 287–295, https://doi.org/10.1002/clen.201400059.
[54] Li Wu, Muller Lan, Chen Niazi, Zheng Xu, Li Chu, Wang Yuan, Unraveling sorption of lead in aqueous solutions by chemically modified biochar derived from coconut fiber: A microscopic and spectroscopic investigation, Sci. Total Environ. 576 (2017) 766–774, https://doi.org/10.1016/j.scitotenv.2016.10.163.
[55] Su Wu, Chai Dai, Development of montmorillonite-supported nano CaO_2 for enhanced dewatering of waste-activated sludge by synergistic effects of filtration aid and peroxidation, Chem. Eng. J. 307 (2017) 418–426, https://doi.org/10.1016/j.cej.2016.08.096.
[56] Xiong Xie, Li Li, Tong Yang, Insight into n-CaO(2)/SBC/Fe(II) Fenton-like system for glyphosate degradation: pH change, iron conversion, and mechanism, J. Environ. Manag. 333 (2023), 117428, https://doi.org/10.1016/j.jenvman.2023.117428.
[57] Yu Xiong, Tsang Cao, Ok Zhang, A review of biochar-based catalysts for chemical synthesis, biofuel production, and pollution control, Bioresour. Technol. 246 (2017) 254–270, https://doi.org/10.1016/j.biortech.2017.06.163.
[58] Xu Xu, Zheng Qiao, Yang Xie, Stimulated biodegradation of all alkanes in soil, Chemosphere 278 (2021), 130444, https://doi.org/10.1016/j.chemosphere.2021.130444.
[59] Ma Yan, Zhang Cao, Liu, Qian Zhou, Identifying the reducing capacity of biomass derived hydrochar with different post-treatment methods, Sci. Total Environ. 643 (2018) 486–495, https://doi.org/10.1016/j.scitotenv.2018.06.232.
[60] Liu Yang, Chen Su, Lin Lin, Bioremediation capability evaluation of benzene and sulfolane contaminated groundwater: Determination of bioremediation parameters, Sci. Total Environ. 648 (2019) 811–818, https://doi.org/10.1016/j.scitotenv.2018.08.208.
[61] Yu Yang, Chen Cho, Shang Tsang, Wang, Ok Yip, Tin-Functionalized Wood Biochar as a Sustainable Solid Catalyst for Glucose Isomerization in Biorefinery, ACS Sustain. Chem. Eng. 7 (5) (2019) 4851–4860, https://doi.org/10.1021/acssuschemeng.8b05311.
[62] Li Zhang, Xu Xing, Adsorption of potentially toxic elements in water by modified biochar: a review, J. Environ. Chem. Eng. 8 (4) (2020), https://doi.org/10.1016/j.jece.2020.104196.
[63] Wei Zhang, He Metz, Long Alvarez, Persistent free radicals in biochar enhance superoxide-mediated Fe(III)/Fe(II) cycling and the efficacy of CaO_2 Fenton-like treatment, J. Hazard Mater. 421 (2022), 126805, https://doi.org/10.1016/j.jhazmat.2021.126805.
[64] Yu Zhao, Ma, Wu Wang, Sodium alginate/graphene oxide hydrogel beads as permeable reactive barrier material for the remediation of ciprofloxacin-contaminated groundwater, Chemosphere 200 (2018) 612–620, https://doi.org/10.1016/j.chemosphere.2018.02.157.
[65] Anwar Zhou, Huang, Liu Guo, Response of antibiotic resistance genes and microbial niches to dissolved oxygen in an oxygen-based membrane biofilm reactor during greywater treatment, Sci. Total Environ. 833 (2022), 155062, https://doi.org/10.1016/j.scitotenv.2022.155062.
[66] Li Zhou, Song Zhao, Yang Huang, Phosphorus immobilization by the surface sediments under the capping with new calcium peroxide material, J. Clean. Prod. (2020) 247, https://doi.org/10.1016/j.jclepro.2019.119135.